Theory of (d, p) and (p, d) reactions including breakup: Comparison of methods

A. M. Moro,[1] F. M. Nunes,[2,3] and R. C. Johnson[2,4]

[1]*Departamento de FAMN, Universidad de Sevilla, Apartado 1065, E-41080 Sevilla, Spain*

[2]*National Superconducting Cyclotron Laboratory, Michigan State University, East Lansing, Michigan 48824, USA*

[3]*Department of Physics and Astronomy, Michigan State University, East Lansing, Michigan 48824, USA*

[4]*Department of Physics, University of Surrey, Guildford GU2 7XH, United Kingdom*

There is an increasing interest in studying transfer reactions to probe the nuclear structure of exotic nuclei. For these loosely bound systems, the role of the continuum needs to be well understood. In this study, we concentrate on (p, d) and (d, p) reactions and compare two formulations for the transfer process that take into account breakup states. Applications to $^{11}\mathrm{Be}(p, d)^{10}\mathrm{Be}$ at $E_{\mathrm{lab}} = 38.4$ MeV/nucleon and $^{10}\mathrm{Be}(d, p)^{11}\mathrm{Be}$ at $E_{\mathrm{lab}} = 12.5$ MeV/nucleon are presented, as is a detailed discussion of convergence rates.

I. INTRODUCTION

Progress in the production of rare isotope beams has opened new avenues for detailed studies of the structure of exotic nuclei. These studies often involve transfer reactions in inverse kinematics as they provide a flexible tool to determine the angular momentum and spectroscopic strength of a number of states [1]. Reactions on light targets, such as (d, p), are of particular experimental interest because the Coulomb barrier is minimized. Recent measurements have mostly focused on light nuclei [2–6], but interest in the heavier isotopes is increasing [7,8].

Given the rising experimental programs involving transfer reactions, focused theoretical efforts have revisited the topic, addressing issues such as the dependence on the optical potentials, coupling effects, and single-particle parameters [9–14].

As one moves away from stability, the role of the continuum in low-energy nuclear reactions needs to be better understood. Deuterons are themselves loosely bound, and deuteron breakup was early identified as an important ingredient in the description of transfer reactions [15–19]. In Ref. [15], an adiabatic theory for elastic deuteron scattering and transfer reactions was derived that is nonperturbative and includes the effects of coupling to deuteron breakup channels. The modifications introduced for (d, p) and (p, d) calculations were particularly simple and amounted to a prescription for calculating the distorting potential in the deuteron channel in a distorted-wave Born approximation (DWBA)-like matrix element in terms of nucleon optical potentials. This differed significantly from the deuteron optical potential and generated breakup contributions, which went far beyond the Born approximation.

Johnson and Soper's calculation of deuteron elastic scattering was a continuum discretized coupled channel (CDCC) calculation in which the continuum of breakup channels was represented by a single channel. The generalized CDCC method is a powerful tool for including breakup channels in the reaction mechanism [20,21]. It is also nonperturbative and does not make use of the adiabatic approximation; however, it is computationally expensive. There have been

a few applications of CDCC to transfer reactions (e.g., Refs. [5,22–26]), and results demonstrate the variety of phenomena that can be addressed within this same framework. While new developments of the CDCC method are taking place [27–29], here we would like to focus on a better understanding of the transfer matrix element when breakup is included.

Starting from a given three-body Hamiltonian, there are many ways of writing the amplitude for $A(p, d)B$ or $B(d, p)A$, including projectile excitation and breakup. Of these, a preference exists for those methods that can be generalized to the actual many-body case of interest and that can be used to extract nuclear structure information with a minimal uncertainty associated with the treatment of three-body dynamics. However, numerical difficulties should also be considered. In the present work, we compare two specific methods.

In Ref. [30], a method is developed for $A(p, d)B$ and $B(d, p)A$, where $A = B + n$ is a weakly bound system, using the adiabatic approximation for both the excitation of the exotic nucleus A and the breakup of the deuteron. This leads to a calculation of the transfer matrix element that is similar to a DWBA calculation, but where the distorted waves are not related to elastic scattering of the composite particle. One important feature of the method introduced in Ref. [30] is that the transfer operator contains only the short-range V_{np} interaction. This focuses attention on the value of the three-body wave function at small n-p separations, where it may be simpler to calculate the full three-body $A + n + p$ wave function. Natural extensions of the model [30] are to include a CDCC wave function for the halolike system, avoiding the adiabatic approximation, and a CDCC wave function for the deuteron, no longer needing the Johnson and Soper simplification [15] or its finite-range extension [19].

Another way of calculating the transfer amplitude is by considering the folding potential of the projectile's constituents and the target as the main distorting field [31]. This is the natural choice in a CDCC formulation because it corresponds to the diagonal coupling potential appearing in the those coupled equations [20]. In this case, the operator in the transfer matrix element can no longer be reduced to V_{np}.

If the CDCC wave function is a good representation of the full three-body wave function in the region of space

contributing to the transfer matrix element, then the fully converged results should provide the correct transition amplitude. CDCC calculations involving rearrangement channels can become very cumbersome, and in some cases, a fully converged solution may not be feasible (e.g., Ref. [32]).

The key questions addressed in this work are as follows:

(i) For a given three-body Hamiltonian, are there significant differences between the predictions of transfer cross sections using different forms of the matrix element when CDCC expansions of the three-body wave functions are used?

(ii) What are the limitations of the CDCC expansion as a way of representing the full solution of the three-body Schrödinger equation?

(iii) Are there any important computational advantages in using specific forms of the transfer amplitude?

(iv) All our calculations are based on a three-body model and hence necessarily involve a simplification of the many-body problem that is the real interest of nuclear structure theory. Does the necessity of linking the three-body model to a many-body theory pick out one of the alternative formulations as being of primary interest?

Our approach is to seek the answers to these questions in the context of selected reactions involving a halo nucleus for which there are data, namely, ^{11}Be$(p,d)^{10}$Be at $E_{\text{lab}} = 38.4$ MeV/nucleon [2] and ^{10}Be$(d,p)^{11}$Be at $E_{\text{lab}} = 12.5$ MeV/nucleon [33].

The article is organized in the following way: The theoretical background is given in Sec. II, results are presented and discussed in Sec. III, and conclusions are drawn in Sec. IV.

II. THREE-BODY MODEL OF (p,d) AND (d,p) REACTIONS

We consider the reaction $A(p,d)B$. Our starting point is a three-body model Hamiltonian,

$$H = K + V_{np} + V_{nB} + U_{pB}, \qquad (1)$$

where K is the total kinetic energy operator, V_{np} is the proton-neutron interaction, V_{nB} is the neutron-B interaction, and U_{pB} is the proton-B interaction. We use the notation V for real potentials and U for complex potentials. We assume that V_{nB} is real because we are interested in transfers from bound neutron states in a real well, and we want all our calculations to derive from a fixed Hamiltonian.

Because of the limitations of the CDCC approximation for the three-body wave function, transfer amplitudes cannot be evaluated by examining the CDCC wave function in the appropriate asymptotic region. There are, however, various ways of expressing the transition amplitude for the reaction $A(p,d)B$ as a matrix element involving the exact solution of the three-body Schrödinger equation in finite regions of configuration space only. An exact prior form amplitude for this process is given by

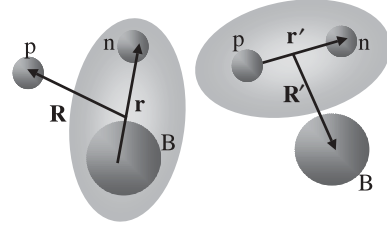$$T_{\text{prior}} = \langle \Psi_{dB}^{(-)} | V_{np} + U_{pB} - U | \Phi_{pA}^{(+)} \rangle, \qquad (2)$$

FIG. 1. Coordinates used for the entrance and exit channels of the transfer reaction $A(p,d)B$.

where $\Psi_{dB}^{(-)}$ is the exact (three-body) wave function with incoming boundary conditions corresponding to the final channel. The initial wave function $\Phi_{pA}^{(+)}$ is defined in terms of an auxiliary potential U, which may be complex and is the solution of

$$[E + i\epsilon - K_{\mathbf{r}} - K_{\mathbf{R}} - V_{nB} - U]\Phi_{pA}^{(+)}(\mathbf{r}, \mathbf{R})$$
$$= +\iota\epsilon\phi_A(\mathbf{r}) \exp(\iota \mathbf{K}_p \cdot \mathbf{R}), \qquad (3)$$

where $\mathbf{r}$ and $\mathbf{R}$ are the n-B and p-A Jacobi coordinates defined in Fig. 1, $\mathbf{K}_p$ is the incident proton momentum, and ϕ_A is the initial n-B bound state. It is important to emphasize that whatever the choice of the auxiliary potential U, the three-body Hamiltonian remains the same.

In Sec. II A, we first examine the formalism for two selected choices of U in the prior form matrix element Eq. (2). In Sec. II B, we extend our study to post form matrix elements.

A. Dependence of the prior form T matrix on U

1. The choice $U = U_{pB}$

If $\Psi_{dB}^{(-)}$ and $\Phi_{pA}^{(+)}$ are exact solutions of their respective three-body Schrödinger equations, the expression in Eq. (2) is independent of U for a wide class of possible choices of U. The form of the T matrix for specific choices of U may suggest certain approximations to the three-body wave functions, instead of the full solution.

Goldberger and Watson [34] introduce the choice $U = U_{pB}(\mathbf{R}_{pB})$ in Eq. (2), which was also the choice of Timofeyuk and Johnson [30]. With this choice, Eq. (2) becomes

$$T_{\text{prior}}(V_{np}) = \langle \Psi_{dB}^{(-)} | V_{np} | \tilde{\Phi}_{pA}^{(+)} \rangle. \qquad (4)$$

A derivation of this matrix element from the three-body Alt, Grassberger, and Sandhas (AGS) equations [35] can be found in Ref. [36].

From Eq. (3), we can see that the initial wave function $\tilde{\Phi}_{pA}^{(+)}$ in Eq. (4) is the solution of the three-body Hamiltonian with V_{np} removed:

$$[E + i\epsilon - K_{\mathbf{r}} - K_{\mathbf{R}} - V_{nB} - U_{pB}]\tilde{\Phi}_{pA}^{(+)}(\mathbf{r}, \mathbf{R})$$
$$= +\iota\epsilon\phi_A(\mathbf{r}) \exp(\iota \mathbf{K}_p \cdot \mathbf{R}). \qquad (5)$$

Note that in the limit $m_n/M_B \to 0$, when recoil effects are negligible, $\tilde{\Phi}_{pA}^{(+)}$ becomes a product of the initial bound-state neutron wave function in A and a proton scattering wave on a target A but is distorted by the potential U_{pB}. Recoil effects that excite A were discussed by Timofeyuk and Johnson [30]

and are referred to as recoil excitation and breakup (REB) effects.

In Ref. [30], the following advantages of using Eq. (4) to calculate T_{prior} were emphasized: (i) Only nucleon-B potentials are needed as input, unlike for the standard DWBA amplitude, for which an optical potential that fits deuteron elastic scattering and an optical potential for $p + A$ is required, and (ii) V_{np}, the interaction that appears in the matrix element is short ranged, which means that $\Psi_{dB}^{(-)}$ is only needed within the range of the n-p interaction. The obvious disadvantage is that there is no simple separation of coordinates in $\tilde{\Phi}_{pA}^{(+)}$, and thus the solution of Eq. (5) is not trivial, except for heavy targets.

In Ref. [30], further simplifications were made in the calculation of Eq. (4). As mentioned in Sec. I, the wave function $\Psi_{dB}^{(-)}$, which contains both elastic deuteron scattering and breakup, is treated using the adiabatic method of Johnson and Soper [15,16] with finite-range corrections included, as discussed by Wales and Johnson [19]. The function $\tilde{\Phi}_{pA}^{(+)}$, which contains components describing elastic, inelastic, and breakup of A by the incident proton, was also calculated within an adiabatic approximation [17,37]. Under these two approximations, the transfer amplitude has a structure similar to a DWBA matrix element, tremendously simplifying the calculations, but the distorted waves are not the usual elastic scattering wave functions, as in DWBA. It is important to realize that despite this formal similarity to DWBA, no Born approximation is involved in the derivation of those expressions. In the present work, we use Eq. (4) without making the preceding approximations. Instead, we replace the three-body wave functions, $\Psi_{dB}^{(-)}$ and $\tilde{\Phi}_{pA}^{(+)}$, by their CDCC approximations, which we discuss in Sec. II C.

2. The choice $U = U_{pA}^{\text{fold}}$

Another possible choice for the auxiliary potential is the folded potential, defined by

$$U_{pA}^{\text{fold}}(\mathbf{R}) = \langle \phi_{nB} | V_{np} + U_{pB} | \phi_{nB} \rangle. \tag{6}$$

This is the diagonal coupling in the CDCC equations [20] for $\Phi_{pA}^{(+)}$ and thus is a natural choice when the CDCC method is used. As this potential depends only on $\mathbf{R}$, the wave function $\Phi_{pA}^{(+)}$ has the factorized form

$$\Phi_{pA}^{(+)}(\mathbf{r}, \mathbf{R}) = \chi_{pA}^{(+)}(\mathbf{R}) \phi_A(\mathbf{r}) \tag{7}$$

and describes elastic scattering of an incident proton on the target A, distorted by a folding potential U^{fold}.

The exact T matrix in this case is

$$T_{\text{prior}}^{\text{fold}} = \langle \Psi_{dB}^{(-)} | V_{np} + U_{pB} - U_{pA}^{\text{fold}} | \chi_{pA}^{(+)} \phi_{nB} \rangle. \tag{8}$$

It is important to notice that the use of U^{fold} to calculate $\chi_{pA}^{(+)}(\mathbf{R})$ does not imply an approximation: In fact, Eq. (8) is exact if $\Psi_{dB}^{(-)}$ is the exact three-body wave function. In our applications, we take the CDCC approximation to this wave function, as in Sec. II A 1.

Here, again, no additional potentials are introduced, and thus the problem is fully determined by the initial three-body Hamiltonian. The main advantage of this method over $T_{\text{prior}}(V_{np})$ is the simplification in $\Phi_{pA}^{(+)}$. The disadvantage resides in the complicated operator $U_{pB} - U_{pA}^{\text{fold}}$, which enhances the nonlocality of this matrix element.

B. Dependence of the post form T matrix on U

The three-body Schrödinger equation can be used to transform the transition matrix element Eq. (2) into its post form, which also involves an auxiliary potential U. This will be referred to as T_{post} and is given by

$$T_{\text{post}} = \langle \Phi_{dB}^{(-)} | V_{nB} + U_{pB} - U | \Psi_{pA}^{(+)} \rangle, \tag{9}$$

where $\Psi_{pA}^{(+)}$ is the exact solution of the three-body Schrödinger equation corresponding to a plane wave proton incident on A and outgoing waves in all other channels, and where $\Phi_{dB}^{(-)}$ satisfies

$$[E - i\epsilon - K_{\mathbf{r}'} - K_{\mathbf{R}'} - V_{np} - U^*]\Phi_{dB}^{(-)}(\mathbf{r}', \mathbf{R}')$$
$$= -\iota\epsilon\phi_d(\mathbf{r}') \exp(\iota\mathbf{K}_d \cdot \mathbf{R}'). \tag{10}$$

As in Sec. II A, we test the dependence in the calculation of the transition amplitude in Eq. (9) on the auxiliary potential by comparing results for two choices of U.

1. The choice $U = U_{pB}$

This case is the analog of the Timofeyuk-Johnson $T_{\text{prior}}(V_{np})$. Here the binding potential in the initial state appears as the transition operator in the matrix element. The T matrix is

$$T_{\text{post}}(V_{nB}) = \langle \tilde{\Phi}_{dB}^{(-)} | V_{nB} | \Psi_{pA}^{(+)} \rangle. \tag{11}$$

The potential V_{nB} does not appear in the equation satisfied by final-state wave function

$$[E - i\epsilon - K_{\mathbf{r}'} - K_{\mathbf{R}'} - V_{np} - U_{pB}^*]\tilde{\Phi}_{dB}^{(-)}(\mathbf{r}', \mathbf{R}')$$
$$= -\iota\epsilon\phi_d(\mathbf{r}') \exp(\iota\mathbf{K}_d \cdot \mathbf{R}'). \tag{12}$$

The state $\tilde{\Phi}_{dB}^{(-)}$ describes a nonphysical situation in which the neutron and proton in the outgoing deuteron interact with each other, but only the proton interacts with B. Nevertheless, if $\Psi_{pA}^{(+)}$ is represented by an accurate solution of the three-body Schrödinger equation, the results obtained with Eq. (11) should be the same as those from Eq. (4).

2. The choice $U = U_{dB}^{\text{fold}}$

Similarly to the prior case, one can choose the folding potential U_{dB} as the auxiliary potential:

$$U_{dB}^{\text{fold}}(\mathbf{R}') = \langle \phi_d | V_{nB} + U_{pB} | \phi_d \rangle. \tag{13}$$

This is the diagonal coupling in the CDCC equations [20] for $\Phi_{dB}^{(+)}$ and therefore corresponds to a standard choice when CDCC is used in the post form of the transition amplitude. Because U_{dB}^{fold} does not depend on $\mathbf{r}'$, $\Psi_{dB}^{(-)}$ factorizes in a distorted wave and the deuteron ground state. The post form

T matrix is then given by

$$T_{\text{post}}^{\text{fold}} = \langle \chi_{dB}^{(-)} \phi_{np} | V_{nB} + U_{pB} - U_{dB}^{\text{fold}} | \Psi_{pA}^{(+)} \rangle, \qquad (14)$$

where $\chi_{dB}^{(-)}$ is the deuteron distorted wave associated with the potential $U_{dB}^{\text{fold}}(\mathbf{R}')$. This matrix element is exact if the initial three-body wave function $\Psi_{pA}^{(+)}$ is exact. In our applications, we use the CDCC approximation to calculate $\Psi_{pA}^{(+)}$.

Even though there are formal similarities between Eq. (8) and Eq. (14), the difference in the operator produces a tremendous difference in the model space needed for convergence. First, the binding potential appearing in the prior form (V_{np}) has a much shorter range than that appearing in the post form (V_{nB}). Second, the operator $U_{pB} - U_{pA}^{\text{fold}}$ in $T_{\text{prior}}(\text{fold})$ is rather different from $U_{pB} - U_{dB}^{\text{fold}}$ in $T_{\text{post}}(\text{fold})$. The difference between deuteron and proton potentials is much more significant than the difference between proton potentials of neighboring nuclei (even if A is a halo). For these two reasons, we can expect nonlocality effects in the transfer matrix elements to be more important in $T_{\text{post}}(\text{fold})$ than in $T_{\text{prior}}(\text{fold})$.

C. Using CDCC for the three-body wave function

All the T matrices in this article are calculated using the CDCC method [20]. More specifically, in the case of the prior form matrix elements introduced earlier, both $\Psi_{dB}^{(-)}$ and $\tilde{\Phi}_{pA}^{(+)}$ in Eq. (4) are obtained using the CDCC expansion and by solving the CDCC coupled channel equation, and the same CDCC solution for $\Psi_{dB}^{(-)}$ is used in Eq. (8). For the post form matrix elements, CDCC expansions are used for $\tilde{\Phi}_{dB}^{(-)}$ and $\Psi_{pA}^{(+)}$ in Eq. (11) and $\Psi_{pA}^{(+)}$ in Eq. (14).

In the CDCC method, the exact wave function $\Psi_{dB}^{(-)}$ appearing in both Eqs. (4) and (8) is replaced by an expansion in terms of a truncated and discretized set of eigenstates of the n-p Hamiltonian $K_{\mathbf{r}'} + V_{np}(\mathbf{r}')$. The coefficients in the expansion are determined from a coupled-channel version of the equation

$$[E - K_{\mathbf{r}'} - K_{\mathbf{R}'} - V_{np} - V_{nB} - U_{pB}^*]\Psi_{dB}^{(-)}(\mathbf{r}', \mathbf{R}') = 0, \quad (15)$$

with the boundary condition that there be a plane wave in the deuteron channel and incoming scattered waves in all other channels. $\tilde{\Phi}_{dB}^{(-)}$ is obtained in a similar way, but with V_{np} removed from Eq. (15).

Similarly, in Eqs. (11) and (14), the exact initial-state wave function $\Psi_{pA}^{(+)}$ is replaced by an expansion in eigenstates of the n-B system, with Hamiltonian $K_{\mathbf{r}} + V_{nB}(\mathbf{r})$. The solutions approximately satisfy

$$[E - K_{\mathbf{r}} - K_{\mathbf{R}} - V_{np} - V_{nB} - U_{pB}]\tilde{\Psi}_{pA}^{(+)}(\mathbf{r}, \mathbf{R}) = 0, \quad (16)$$

with the boundary condition that there be a plane wave in the incoming proton channel and outgoing scattered waves in all other channels. Again, $\tilde{\Phi}_{pA}^{(+)}$ is calculated using the preceding equation with V_{nB} removed.

The CDCC functions for the initial $p + A$ state and final $d + A$ state involve expansions in different complete sets and depend on different Jacobi coordinates; therefore we expect

TABLE I. Optical potentials used in our applications.

	E_{beam} (MeV)	V_0 (MeV)	r_0 (fm)	a_0 (fm)	W_v (MeV)	W_d (MeV)	r_i (fm)	a_i (fm)
p-^{10}Be	38.4	51.2	1.114	0.57	19.5	0	1.114	0.50
p-^{10}Be	12.5	68.461	1.188	0.469	0	15.629	1.043	0.328
n-^{10}Be		51.639	1.39	0.52				
n-p		72.15		1.484				

the sizes of the model spaces to be different in the various methods: $T_{\text{prior}}(V_{np})$ and $T_{\text{post}}(V_{nB})$, $T_{\text{prior}}(\text{fold})$ and $T_{\text{post}}(\text{fold})$.

Regarding the methods described by Eq. (4) and Eq. (11), one might naively think that there is double counting of the three-body continuum because there are CDCC discretizations for both initial and final states. This is not the case. The two states involve different three-body Hamiltonians in a matrix element, which emphasizes a particular subspace of the six-dimensional coordinate space. The full three-body Schrödinger equation guarantees that the overlaps of these functions, when evaluated as in Eq. (4) and Eq. (11), produce the correct transition amplitude.

III. RESULTS

We first consider the reaction ^{11}Be(p,d)^{10}Be at $E_{\text{lab}} = 38.4$ MeV/nucleon. Table I contains the parameters for all interactions used in this application, where V_0, r_0, and a_0 are the depth, radius, and diffuseness of the real part, respectively; W_v, W_d, r_i, and a_i are the depth of the volume and surface imaginary potentials and their radius and diffuseness, respectively. For $p + {}^{10}$Be, we use an optical potential of Woods-Saxon shape, which reproduces elastic scattering at $E_{\text{lab}}/A = 39.1$ MeV [38]. (In our formulation, the Hamiltonian is energy-independent; thus this is a reasonable choice for the reactions under study, although not unique.) The $n + {}^{10}$Be interaction is obtained fixing the diffuseness and the radius and adjusting the depth to reproduce a $2s$ state with the correct neutron separation energy ($S_n = 0.504$ MeV). For the deuteron, we use a central Gaussian interaction, reproducing the binding energy and the radius of the ground state of the n-p system.

All calculations are performed using the code FRESCO [39]. For the purpose of our study, interactions need to be sensible and qualitatively relate to the physical systems. However, as the objective of this work is not to extract precise structure information, but rather to compare different reaction methods, spin dependence or tensor terms in the interactions would be an unnecessary complication. Also, the $n + {}^{10}$Be interaction (V_{nB}) appearing in the matrix operator of Eq. (14) needs to be real and independent of angular momentum because of the limitations of the FRESCO implementation.

In Fig. 2, we show the results for the prior form: $T_{\text{prior}}(\text{fold})$ (Fig. 2, top) and $T_{\text{prior}}(V_{np})$ (Fig. 2, bottom). In $T_{\text{prior}}(\text{fold})$, deuteron breakup is included through CDCC in the final state. Convergence of the angular distribution up to 60° is obtained when n-p partial waves up to $l_f = 4$ are included. In $T_{\text{prior}}(V_{np})$, in addition to the CDCC wave function for the

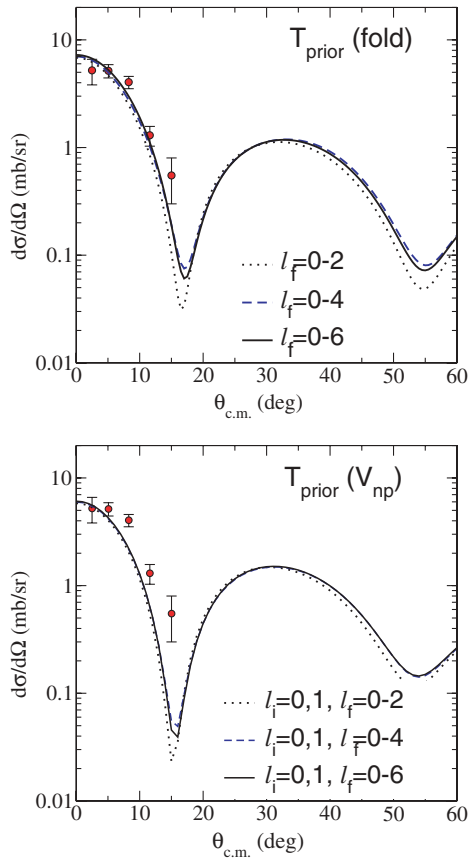FIG. 2. (Color online) Transfer cross sections for ^{11}Be$(p,d)^{10}$Be at $E_p = 38.4$ MeV calculated in the prior form: convergence with respect to the number of partial waves for n-^{10}Be (l_i) and p-n (l_f). Data are taken from Ref. [2].

FIG. 3. (Color online) Transfer cross sections for ^{11}Be$(p,d)^{10}$Be at $E_p = 38.4$ MeV calculated in the post form: convergence with respect to the number of partial waves for n-^{10}Be (l_i) and p-n (l_f). Data are taken from Ref. [2].

deuteron, we also need the CDCC wave function for the entrance channel [see Eq. (4)]. Convergence in l_i (n-^{10}Be partial waves) is rapid and requires only s and p waves. We also have to consider the sum over the projectile-target angular momentum L. Convergence is obtained for $L_{\max} = 25$. As to the radial grid, integration out to 40 fm with steps of 0.1 fm was found sufficient.

Figure 2 shows that the converged angular distributions obtained with $T_{\text{prior}}(\text{fold})$ and $T_{\text{prior}}(V_{np})$ are in very good agreement. We also verified that there were no significant differences in either the size or speed of the calculations.

We now turn our attention to the post representation. In Fig. 3, we present the convergence study for $T_{\text{post}}(\text{fold})$ (Fig. 3, top) and $T_{\text{post}}(V_{nB})$ (Fig. 3, bottom). Within $T_{\text{post}}(\text{fold})$, the ^{11}Be breakup is included through CDCC in the initial state; thus l_i is the relevant quantum number in the expansion. We find that the angular distribution out to 60° reaches convergence for $l_i \leqslant 6$. For $T_{\text{post}}(V_{nB})$, both entrance and exit channels are expressed in terms of CDCC, so convergence with respect to l_i and l_f should be considered [see Eq. (11)]. Full convergence in this case was not feasible. It is clear from Fig. 3 that $l_f = 6$ is still not enough for the outgoing channel, and even though it appears that the calculation has converged with respect to l_i, the model space for the incoming channel might need to be increased if more partial waves are included in the outgoing channel. We
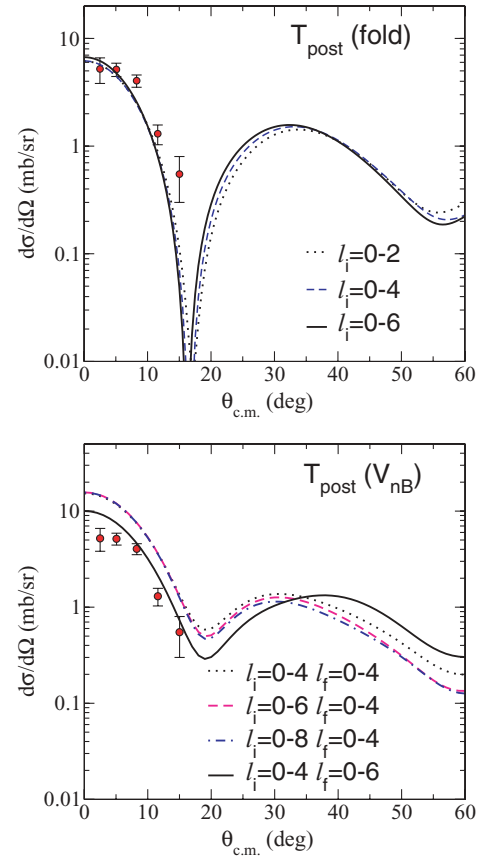
find that the angular distributions for the transfer calculated using $T_{\text{post}}(\text{fold})$ are in reasonable agreement with those using $T_{\text{prior}}(\text{fold})$, particularly at forward angles, which is the region more relevant for the extraction of spectroscopic information. This is to be expected when starting from the same three-body Hamiltonian. The small differences remaining test the level of accuracy of the CDCC representation of the full three-body wave function. The cross sections calculated with $T_{\text{post}}(V_{nB})$ do not agree with $T_{\text{post}}(\text{fold})$. Because the calculations presented for $T_{\text{post}}(V_{nB})$ are not converged, we do not believe that there is physical significance in this difference.

Computationally, the converged $T_{\text{post}}(\text{fold})$ calculation is somewhat more demanding than the converged $T_{\text{prior}}(\text{fold})$ calculation, regarding both speed and memory requirements, because of the need for a larger model space. The $T_{\text{post}}(V_{nB})$ calculation, in addition to the lack of convergence, is by far the most demanding computationally. This result shows how important the choice of the appropriate representation of the transition amplitude can be in practical calculations, despite the formal equivalence between the different representations.

To better understand the characteristics of the matrix elements in these different approaches, we present in Table II the range of nonlocality of the transfer kernels (RNL) required for the four types of calculations as well as a summary of the partial waves used. As $T_{\text{prior}}(V_{np})$ involves only the

TABLE II. Convergence parameters for the different methods, where RNL refers to the range of nonlocality in the transfer couplings (i.e., R-R').

	l_i	l_f	RNL (fm)
Prior(fold)	–	4	14
Prior(V_{np})	1	4	5
Post(fold)	6	–	21
Post(V_{nB})	6	>6	20

V_{np} interaction in the operator, we expect this range to be small as compared with $T_{\text{prior}}(\text{fold})$, which contains the term $U_{pB} - U_{pA}^{\text{fold}}$. This is verified in practice (see Table II). As mentioned in Sec. II B, for the $T_{\text{post}}(V_{nB})$ and $T_{\text{post}}(\text{fold})$ formalisms, instead of V_{np}, the binding potential for n-^{11}Be is used in the operator. Consequently, the range required is much larger than for the prior methods.

As mentioned earlier, we have chosen a central spin-independent effective interaction for the n-^{10}Be system. This interaction does not reproduce the excited $1/2^-$ bound state in ^{11}Be, bound by 0.18 MeV. Using the prior representation, we have checked that this bound state has a negligible effect in the reaction mechanism for this reaction.

In Figs. 2 and 3, we show data along with the theoretical predictions. This serves as an indication that our starting three-body Hamiltonian, Eq. (1), is not too far from reality. We emphasize, however, that we cannot expect our predicted transfer angular distributions to be appropriate for extracting spectroscopic factors or other nuclear structure information. As discussed earlier, in our model, there is no imaginary part in the n-^{10}Be interaction, when in reality, there should be an imaginary component of similar magnitude to the proton optical potential. Also, our calculations implicitly assume a unit spectroscopic factor (norm of the n-^{10}Be overlap function [1]), but it is not obvious what will be the effect on our results if the spectroscopic factor were to differ from this value because then the effective three-body Hamiltonian would need to include core internal degrees of freedom, and several overlap functions might contribute to the process.

We have also studied the ^{10}Be$(d,p)^{11}$Be reaction at $E_d = 25$ MeV. All interactions apart from the proton optical potential are kept the same. The proton optical potential taken at half the deuteron energy (shown in Table I) is the same as that used in Ref. [30]. For the (d,p) case, we have only performed calculations in the post representation. Note that the post form matrix elements for the (d,p) reaction are similar to the prior form matrix elements for the (p,d) reaction. Here we only show the converged results.

For the $T_{\text{post}}(\text{fold})$ calculation, convergence was achieved with $l_i = 0, 2, 4$ partial waves for the p-n continuum, whereas for the $T_{\text{post}}(V_{pn})$ calculation, we needed, in addition, $l_f \leqslant 2$ for the n-^{10}Be continuum. The odd partial waves for the deuteron continuum were found to have a negligible effect on the (d,p) cross section. As expected, the range of nonlocality required for the $T_{\text{post}}(V_{pn})$ calculation (RNL = 5 fm) was significantly smaller than that for the $T_{\text{post}}(\text{fold})$ calculation (RNL = 15 fm). This difference may represent a
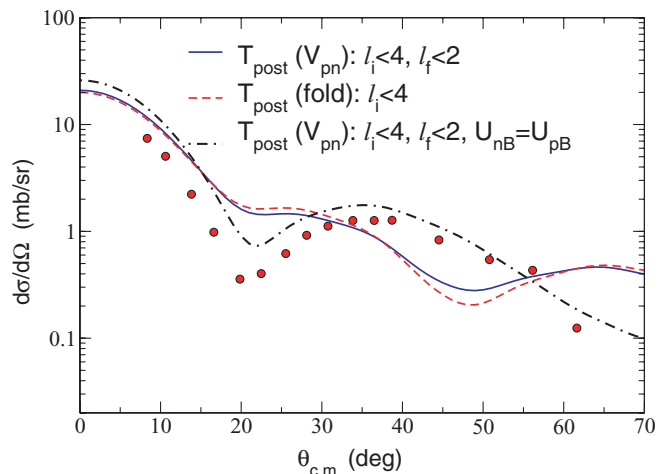

FIG. 4. (Color online) Transfer cross sections for ^{10}Be$(d,p)^{11}$Be at $E_d = 25$ MeV: comparison of $T_{\text{post}}(V_{np})$ and $T_{\text{post}}(\text{fold})$. Data are taken from Ref. [33].

significant numerical advantage of the $T_{\text{prior}}(V_{pn})$ representation in practical calculations. In Fig. 4, we compare the calculations using the two post representations, along with the experimental data from Ref. [33]. The two calculations are in good agreement, but they depart considerably from the data.

At this stage, it is worth recalling that we have restricted ourselves to a very simple Hamiltonian, with only one complex interaction (U_{pB}) and a very simplified description of the ^{11}Be spectrum because of our fixed n-^{10}Be interaction. We have therefore performed another calculation using a complex n-^{10}Be interaction for the incident (deuteron) channel ($U_{nB} = U_{pB}$) and a real parity-dependent interaction for n-^{10}Be in the final state, which is identical to the one in Table I, except for the $\ell = 1$ depth, which is adjusted to reproduce the $1p_{1/2}$ bound state in ^{11}Be. Such a combination of potentials would have made the comparisons in Sec. II impossible. The result of this calculation, using the $T_{\text{post}}(V_{pn})$ formula, is displayed in Fig. 4 with a dash-dotted line. This new calculation brings the shape of the angular distribution in much better agreement with the data, illustrating the dependence of the results on the underlying three-body Hamiltonian.

There have been attempts in the past [40,41] to decide on the relative merits of post- and prior-form DWBA matrix elements by comparison with experiment. We emphasize that none of the calculations reported here are DWBA calculations and that the issues discussed here cannot be decided by comparison with experiment. We address solely the question of accurate and practical evaluation of the predictions of three-body models and which methods are most simply generalized to the many-body case, with the aim of extracting credible nuclear structure information.

IV. CONCLUSIONS

We have found that for the ^{11}Be$(p,d)^{10}$Be reaction, there is very little to choose between the two T matrices $T_{\text{prior}}(V_{np})$ and $T_{\text{prior}}(\text{fold})$ from the point of view of convergence and

convenience. The same can be said about the corresponding post form results for the $^{10}\text{Be}(d,p)^{11}\text{Be}$ reaction. The agreement between converged results implies that within the subspaces of the Jacobi-coordinate six-dimensional space required for the two methods, the CDCC wave functions represent the exact three-body wave functions with similar accuracy. Our study of $^{11}\text{Be}(p,d)^{10}\text{Be}$ using the post form clearly shows the difficulties one might encounter when the transition operator contains interactions with longer range. Our study indicates that for transfer observables, it is best to use the prior form of the matrix elements for (p,d) reactions and the post form for (d,p) reactions.

From the point of view of linking three-body models with the underlying many-body theory, the two matrix elements $T_{\text{prior}}(V_{np})$ and $T_{\text{prior}}(\text{fold})$ have a very different significance [17]. In the many-body generalization of $T_{\text{prior}}(V_{np})$, the fact that V_{np} does not depend on the internal coordinates of the core B (in our case, ^{10}Be) means that nuclear structure information appears entirely through the overlap function $\phi_{AB}(\vec{r}_n)$ of A and B. The question of what nuclear structure information can be deduced from a particular transfer experiment then reduces to the question of what features of ϕ_{AB} (spectroscopic factor, asymptotic normalization constant, etc.) an experiment at a particular incident energy or angular range is sensitive to. The same consideration applies when it is necessary to include excitations of A and/or B in the matrix element because then, additional overlap functions appear.

In the method in which the folding potential is used, $T_{\text{prior}}(\text{fold})$, the transfer matrix element is not as attractive when generalized to the many-body case. Because of the complicated transfer operator in Eq. (8), the matrix element does not involve a single overlap function but, in principle, can involve a large number of overlap functions as well as matrix elements of the many-body interaction V_{pB} between different states of B.

This study is particularly relevant for light systems. As the mass of the target increases, both formalisms $T_{\text{prior}}(V_{np})$ and $T_{\text{prior}}(\text{fold})$ simplify, and the practical differences found in our applications will not arise. For heavy targets, the initial state in $T_{\text{prior}}(V_{np})$ factorizes as in the CDCC approach, and the complicated operator in $T_{\text{prior}}(\text{fold})$ reduces to V_{np}. In this limit, these two approaches become equivalent.

This same $^{11}\text{Be}(p,d)$ reaction has been used for a comparison between CDCC and the solution of the full three-body integral equations (known as the AGS equations) [38]. The calculations here denoted as $T_{\text{prior}}(\text{fold})$ correspond to CDCC-TR* in Ref. [38], apart from minor differences in the interactions. The comparison with Faddeev shows an $\approx 15\%$ difference between the two calculations, demonstrating the level of accuracy of $T_{\text{prior}}(\text{fold})$. Writing the matrix element in terms of the short-range V_{np}, as in $T_{\text{prior}}(V_{np})$, held promise in solving this disagreement because then the CDCC representation of Ψ_{dB} is at its best. However, our present study suggests that there are still inaccuracies, arising probably from the CDCC expansion of the initial state Φ_{pA} because there is no truncation of the matrix element with regard to the n-^{10}Be distance.

[1] I. Thompson and F. Nunes, *Nuclear Reactions for Astrophysics* (Cambridge University Press, Cambridge, 2009).
[2] J. S. Winfield *et al.*, Nucl. Phys. **A683**, 48 (2001).
[3] A. H. Wuosmaa *et al.*, Phys. Rev. Lett. **94**, 082502 (2005).
[4] A. H. Wuosmaa *et al.*, Phys. Rev. C **72**, 061301(R) (2005).
[5] H. B. Jeppesen *et al.*, Phys. Lett. **B642**, 449 (2006).
[6] I. Tanihata *et al.*, Phys. Rev. Lett. **100**, 192502 (2008).
[7] K. L. Jones *et al.*, Phys. Rev. C **70**, 067602 (2004).
[8] J. S. Thomas *et al.*, Phys. Rev. C **76**, 044302 (2007).
[9] X. D. Liu, M. A. Famiano, W. G. Lynch, M. B. Tsang, and J. A. Tostevin, Phys. Rev. C **69**, 064313 (2004).
[10] F. Delaunay, F. M. Nunes, W. G. Lynch, and M. B. Tsang, Phys. Rev. C **72**, 014610 (2005).
[11] A. M. Mukhamedzhanov and F. M. Nunes, Phys. Rev. C **72**, 017602 (2005).
[12] J. Lee, J. A. Tostevin, B. A. Brown, F. Delaunay, W. G. Lynch, M. J. Saelim, and M. B. Tsang, Phys. Rev. C **73**, 044608 (2006).
[13] J. Lee, M. B. Tsang, and W. G. Lynch, Phys. Rev. C **75**, 064320 (2007).
[14] D. Y. Pang, F. M. Nunes, and A. M. Mukhamedzhanov, Phys. Rev. C **75**, 024601 (2007).
[15] R. C. Johnson and P. J. R. Soper, Phys. Rev. C **1**, 976 (1970).
[16] J. D. Harvey and R. C. Johnson, Phys. Rev. C **3**, 636 (1971).
[17] R. C. Johnson, in *Reaction Mechanisms for Rare Isotope Beams*, AIP Conf. Conf. Proc. **79**, 128 (2005).
[18] R. C. Johnson and P. C. Tandy, Nucl. Phys. **A235**, 56 (1974).
[19] G. L. Wales and R. C. Johnson, Nucl. Phys. **A274**, 168 (1976).
[20] M. Kamimura, M. Yahiro, Y. Iseri, H. Kameyama, Y. Sakuragi, and M. Kawai, Prog. Theor. Phys. Suppl. **89**, 1 (1986).
[21] N. Austern, Y. Iseri, M. Kamimura, M. Kawai, G. Rawitscher, and M. Yahiro, Phys. Rep. **154**, 125 (1987).
[22] A. M. Moro, R. Crespo, F. M. Nunes, and I. J. Thompson, Phys. Rev. C **66**, 024612 (2002); **67**, 047602 (2003).
[23] K. Ogata, M. Yahiro, Y. Iseri, and M. Kamimura, Phys. Rev. C **67**, 011602(R) (2003).
[24] M. Iijima, Y. Aoki, A. Ozawa, and N. Okumura, Nucl. Phys. **A793**, 79 (2007).
[25] N. Keeley and R. S. Mackintosh, Phys. Rev. C **77**, 054603 (2008).
[26] N. Keeley and V. Lapoux, Phys. Rev. C **77**, 014605 (2008).
[27] N. C. Summers, F. M. Nunes, and I. J. Thompson, Phys. Rev. C **73**, 031603(R) (2006); **74**, 014606 (2006).

[28] M. Rodríguez-Gallardo, J. M. Arias, J. Gómez-Camacho, R. C. Johnson, A. M. Moro, I. J. Thompson, and J. A. Tostevin, Phys. Rev. C **77**, 064609 (2008).

[29] T. Matsumoto, T. Egami, K. Ogata, Y. Iseri, M. Kamimura, and M. Yahiro, Phys. Rev. C **73**, 051602(R) (2006).

[30] N. K. Timofeyuk and R. C. Johnson, Phys. Rev. C **59**, 1545 (1999).

[31] A. M. Moro and F. M. Nunes, Nucl. Phys. **A767**, 138 (2006).

[32] A. M. Moro, R. Crespo, H. Garcia-Martinez, E. F. Aguilera, E. Martinez-Quiroz, J. Gomez-Camacho, and F. M. Nunes, Phys. Rev. C **68**, 034614 (2003).

[33] B. Zwieglinski, W. Benenson, R. G. H. Robertson, and W. R. Coker, Nucl. Phys. **A315**, 124 (1979).

[34] M. L. Goldberber and K. M. Watson, *Collision Theory* (Dover, New York, 2004), p. 841.

[35] E. O. Alt, P. Grassberger, and W. Sandhas, Nucl. Phys. **B2**, 167 (1967).

[36] R. C. Johnson, Phys. Rev. C **80**, 044616 (2009).

[37] R. C. Johnson, J. S. Al Khalili, and J. A. Tostevin, Phys. Rev. Lett. **79**, 2771 (1997).

[38] A. Deltuva, A. M. Moro, E. Cravo, F. M. Nunes, and A. C. Fonseca, Phys. Rev. C **76**, 064602 (2007).

[39] I. J. Thompson, Comput. Phys. Rep. **7**, 167 (1988).

[40] N. Matsuoka *et al.*, Nucl. Phys. **A391**, 357 (1982).

[41] G. Baur, R. Shyam, F. Rösel, and D. Trautmann, Phys. Rev. C **28**, 946 (1983).